

TI Designs: TIDA-01367

适用于 Cavium 的高功率稳压器参考设计 ThunderX2® Arm® 处理器



说明

此参考设计使用 TPS53679 多相控制器和 CSD95490Q5MC 智能功率级，可用于实现适合为联网专用集成电路 (ASIC) 供电的高性能设计。该控制器的双路输出分别面向具有六相设计的 240A、0.8V 内核轨和 20A、0.85V 辅助轨。智能功率级和集成 PMBus™ 允许方便轻松设置输出电压并遥测关键设计参数。此设计允许对电源进行配置、智能 VID 调整和补偿调整，并可监控输入和输出电压、电流、功率和温度。TI 的 Fusion Digital Power™ Designer 用于对系统进行编程、监控和验证以及确定其特性。

资源

TIDA-01367	设计文件夹
TPS53679	产品文件夹
CSD95490Q5MC	产品文件夹
Fusion Digital Power™ 设计器	产品文件夹



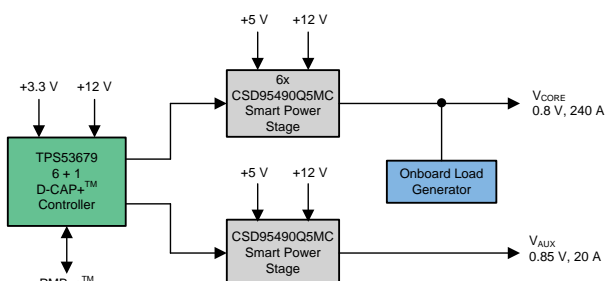
咨询我们的 E2E 专家

特性

- 双轨 6+1 设计 - 高功率内核轨和单相辅助轨
- 内核轨和辅助轨的峰值效率为 90% 和 91%
- D-CAP+™ 调制器可实现出色的电流共享能力和瞬态响应
- 兼容 PMBus，可实现输出电压设置以及 V_{IN} 、 V_{OUT} 、 I_{OUT} 和温度遥测
- 通过 PMBus 实现完整补偿调优
- 提供 $\pm 5\%V_{OUT}$ 目标（具有 150A 阶跃电流）所需的最小输出电容

应用

- 企业交换机
- 企业服务器主板
- 联网 ASIC
- 微服务器
- 网络附加存储



An IMPORTANT NOTICE at the end of this TI reference design addresses authorized use, intellectual property matters and other important disclaimers and information.

1 System Description

The *High-Power Voltage Regulator Reference Design for Cavium ThunderX2® Arm® Processors* is a power-dense, high-performance design targeted at powering complex networking ASICs that can be found anywhere from enterprise switches to server motherboards. The dual-output multiphase controller and TI's proprietary Smart Power Stages allow for an integrated design, which, when compared to more traditional discrete designs, eliminates a number of passive components and reduces the printed-circuit board (PCB) layout area. High-performance networking ASICs require excellent thermal performance, efficiency, and a fast transient response from their voltage regulators while also requiring on-the-fly optimization through PMBus. This design meets all the criteria with a minimal number of output capacitors and a simple thermal solution. Most importantly, a 240-A maximum current on the core rail can be handled with only a six-phase solution while competing vendors may require eight or more phases for the same specifications.

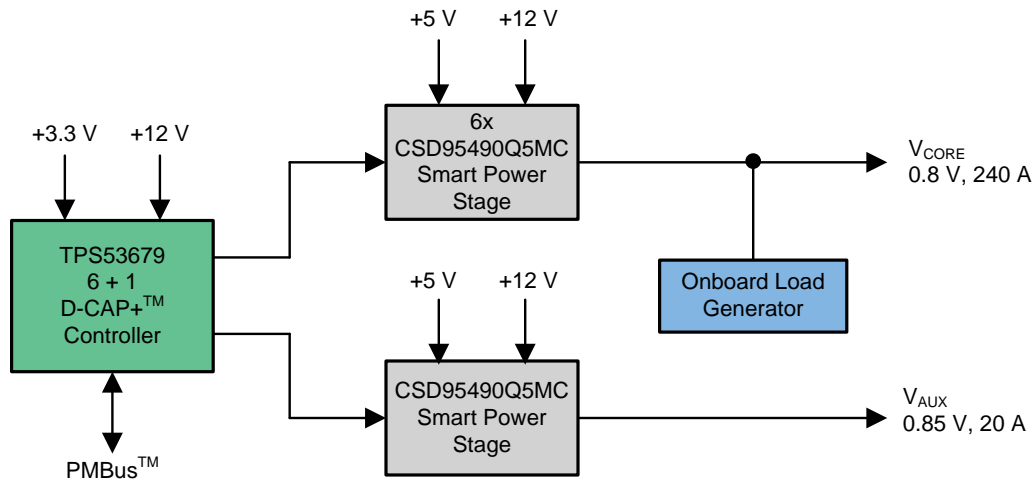
1.1 Key System Specifications

表 1. Key System Specifications

PARAMETER	SPECIFICATIONS
Input supply	12 V, $\pm 5\%$
DC tolerance	$\pm 2\%$
AC tolerance	$\pm 5\%$
Switching frequency	600 kHz
Nominal output voltage – core rail	0.8 V
Max output current – core rail	240 A
TDC current – core rail	200 A
DC load line – core rail	0.5 m Ω
Max load step – core rail	150 A at 500 A/ μ s
Number of phases – core rail	6
Nominal output voltage – aux rail	0.85 V
Max output current – aux rail	20 A
TDC current – aux rail	16 A
DC load line – aux rail	—
Max load step – aux rail	10 A at 20 A/ μ s
Number of phases – aux rail	1

2 System Overview

2.1 Block Diagram



Copyright © 2017, Texas Instruments Incorporated

2.2 Highlighted Products

2.2.1 TPS53679 – Dual-Channel D-CAP+™ Step-Down Multiphase Controller With NVM and PMBus™ for VR13 Server V_{CORE} Applications

- Configurable for 6+1 or 5+2 scenarios
- Programmable loop compensation through PMBus
- Configurable with non-volatile memory (NVM) for low external component counts
- Dynamic phase shedding with programmable current threshold for optimizing efficiency at light and heavy loads
- PMBus™ system interface for telemetry of voltage, current, power, temperature, and fault conditions
- 5 mm × 5 mm, 40-pin, QFN PowerPad™ integrated circuit package

2.2.2 CSD95490Q5MC – 75-A Synchronous Buck NexFET™ Power Stage With DualCool™ Packaging

- 75-A continuous current capability
- 95% system efficiency at 25 A
- Up to 1.25-MHz switching frequencies supported
- Temperature-compensated bidirectional current sense signal
- Analog temperature output and fault monitoring
- High-density, low-inductance, SON 5x6-mm package

2.3 System Design Theory

The D-CAP+ modulator of the TPS53679 controller is integral to the high-performance of this reference design. This modulator allows the control loops of both rails to remain stable over a wide range of operating conditions because the transfer function is insensitive to variations in input voltage, load current, and phase number. Phase margins of 71.1° and 52.7° were measured for the core and auxiliary rails, respectively, with crossover frequencies of 64 kHz and 79 kHz. Placing the unity gain frequencies higher than 1/10 the switching frequencies allows for a faster transient response that can keep V_{OUT} within its regulation limits during large load steps, such as the 150-A step on the core rail. Stability is maintained even as the load current duty cycle and frequency are varied. Compensation can easily be adjusted through the PMBus using TI's Fusion graphical user interface (GUI), which allows the user to easily tune the design for a wide range of output filters, including using all ceramic output capacitors, should the design requirements change. At high load currents, the D-CAP+ modulator can keep all phase currents evenly balanced to avoid thermally stressing or damaging either the field-effect transistors (FETs), inductors, or load while maintaining tight output voltage regulation.

The CSD95490Q5MC Smart Power Stage features an optimized driver-FET solution in a thermally-efficient package that provides high efficiency up to 75 A of DC load current. Higher efficiency means lower power loss and thus excellent thermal performance, which allows for the high current requirements on the core rail to be met with only six phases as opposed to eight or more on competing solutions. Integrated fault monitoring and temperature reports back to the TPS53679 device and complements the PMBus functionality, which allows for operational telemetry, painless debug, validation, and configuration of the design. On-chip bidirectional current sensing offers increased accuracy compared to discrete circuitry and eliminates the requirement to implement and tune a direct current resistance (DCR) or resistor sense passive network.

3 Getting Started Hardware and Software

3.1 Hardware

The hardware for this design is as follows:

- 12-V, 20-A power supply
- 5-V, 1-A power supply
- 500-MHz oscilloscope with differential and passive probes
- Function generator capable of pulse with $< 1\text{-}\mu\text{s}$ rise times (hook to J5 on load transient circuit)
- Digital multimeter
- USB interface adapter EVM

3.2 Software

This design uses TI's Digital Fusion Power Designer software.

3.3 Test Setup

图 1 shows the test setup of this reference design.

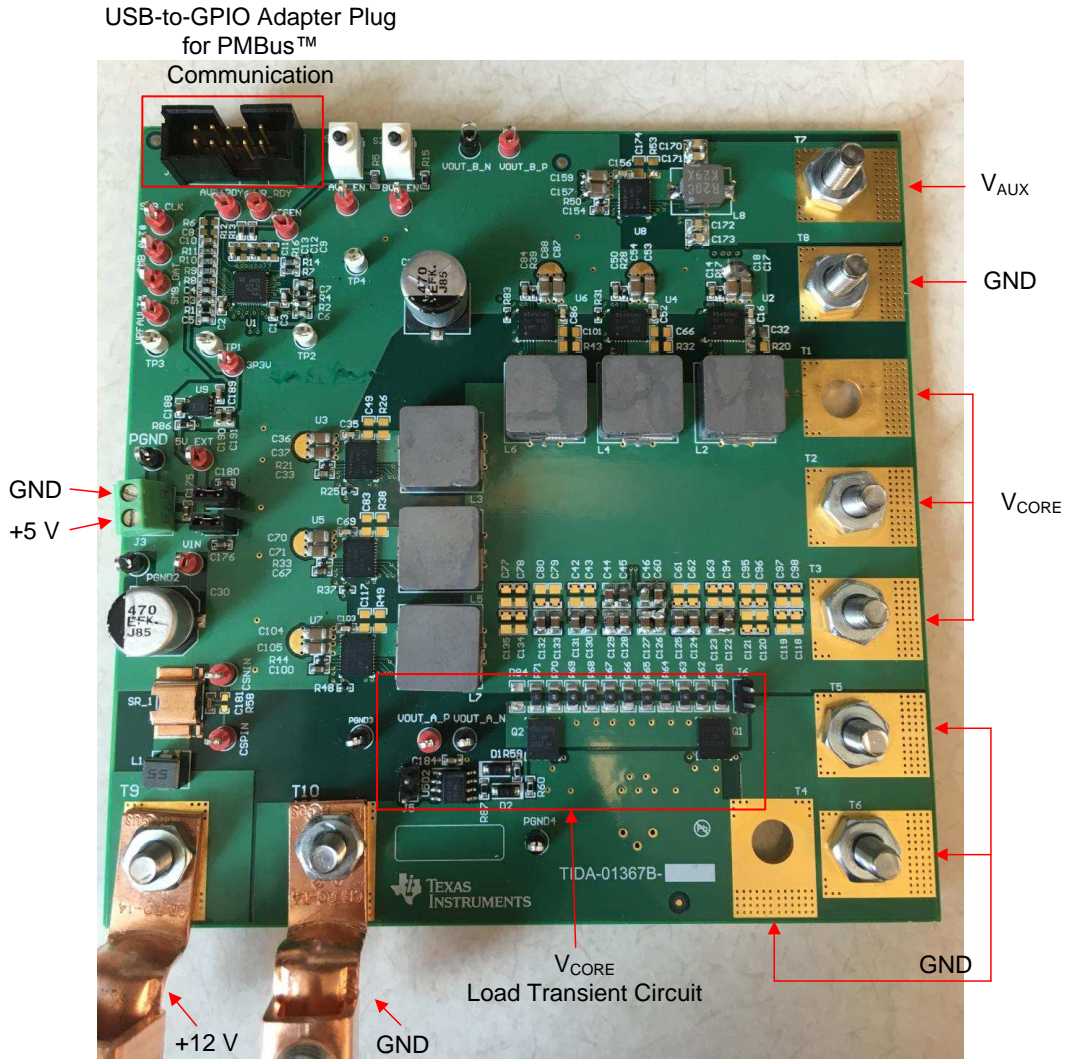


图 1. TIDA-01367 Test Setup

4 Test Results

4.1 Efficiency and Power Loss

For the core rail, a peak efficiency of 89.6% was measured at the target output voltage of 0.8 V at 45 A of load current (see 图 2, 图 3). An 85.1% efficiency was measured at the 200-A thermal design current (TDC). At an output voltage of 1 V, the peak efficiency of 91.1% came at 50 A while the TDC efficiency was 86.7%. Both curves include the inductor losses and VDD rail losses of the CSD95490Q5MC power stages. The full 240-A efficiency curve cannot be taken due to the max current capability of the electronic load rolling off for loads of 190 A to 200 A at output voltages less than 1 V. During testing, the DC loadline of this rail was disabled to get the high possible current range from the load.

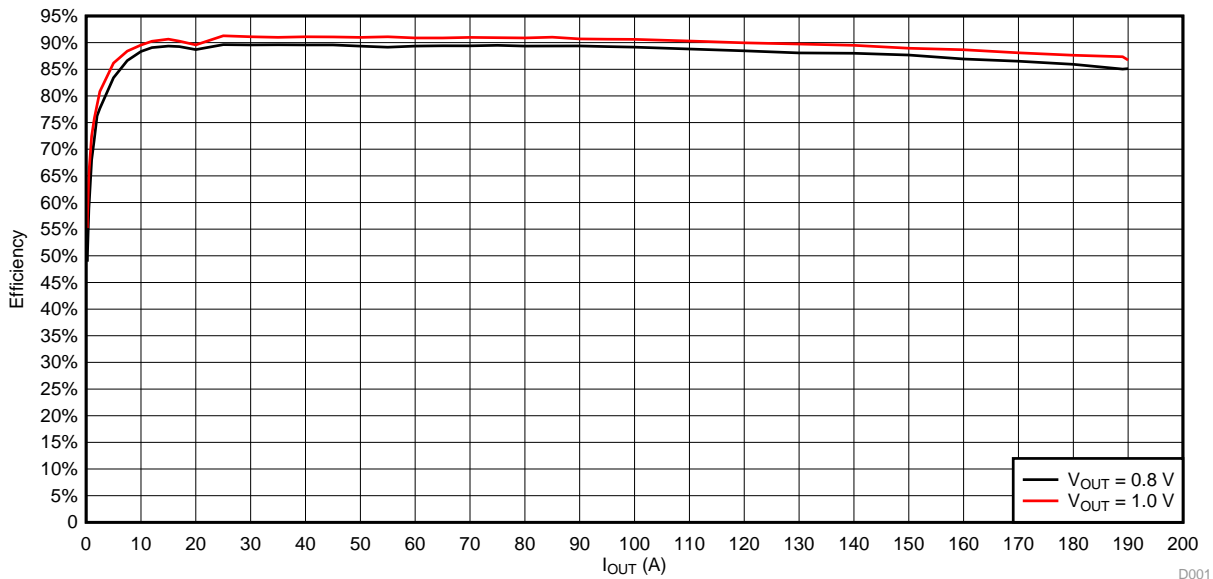


图 2. Core Rail Efficiency

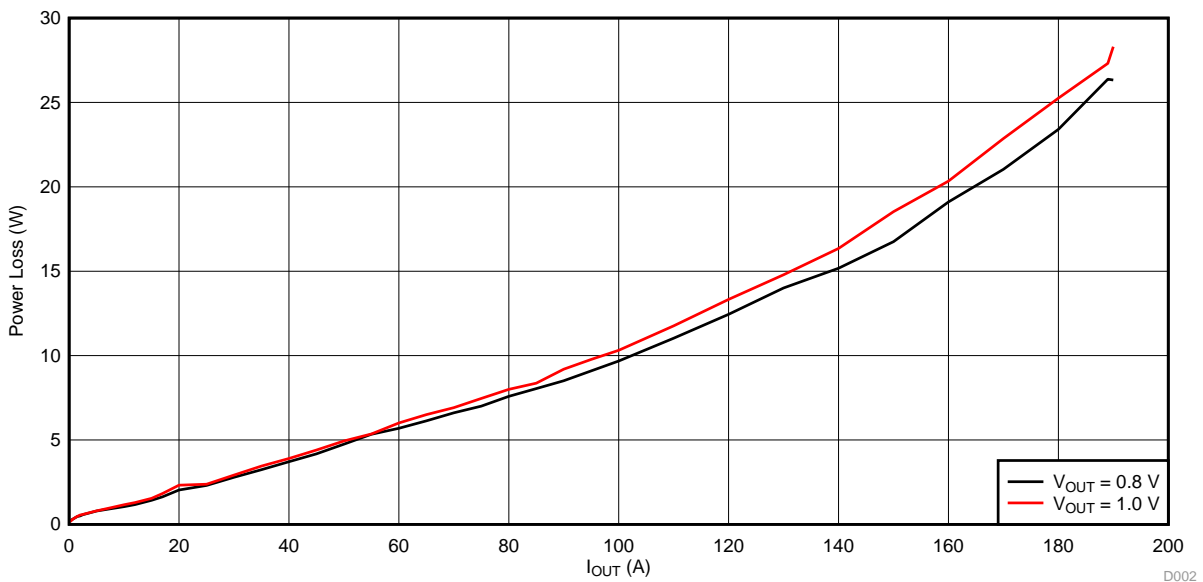


图 3. Core Rail Power Loss

Efficiency measurements on the single-phase auxiliary rail were more straightforward and a full 20-A curve was taken (see 图 4, 图 5). The inductor and VDD power stage loss are included in the results. A peak efficiency of 91% was measured at a load of 9 A and the 16-A TDC efficiency was 89.9% for an output voltage of 0.85 V.

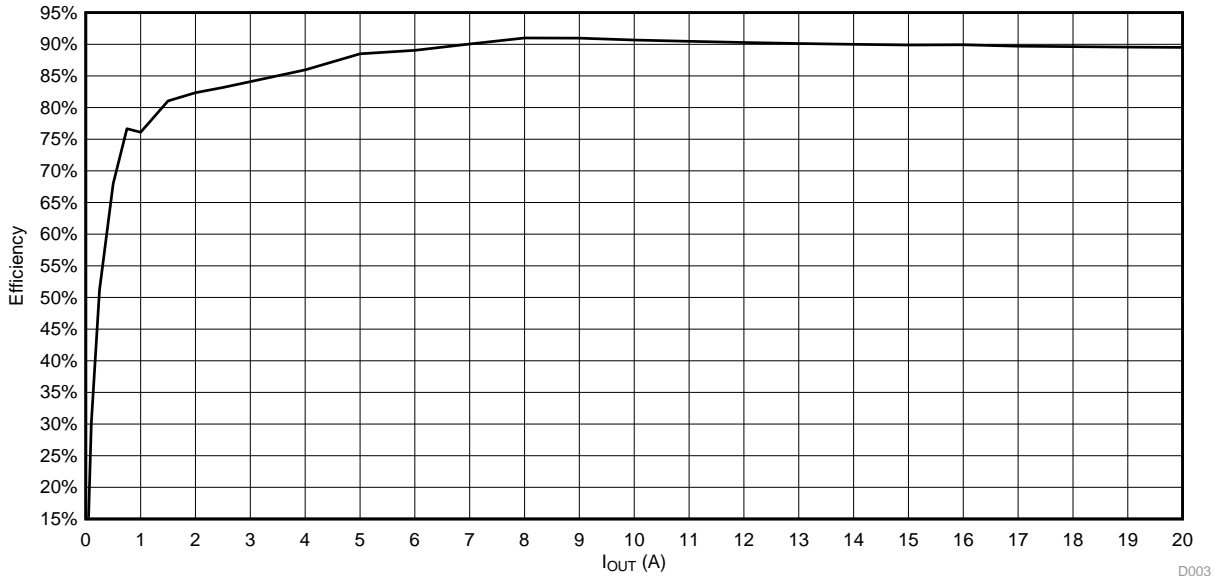


图 4. Auxiliary Rail Efficiency

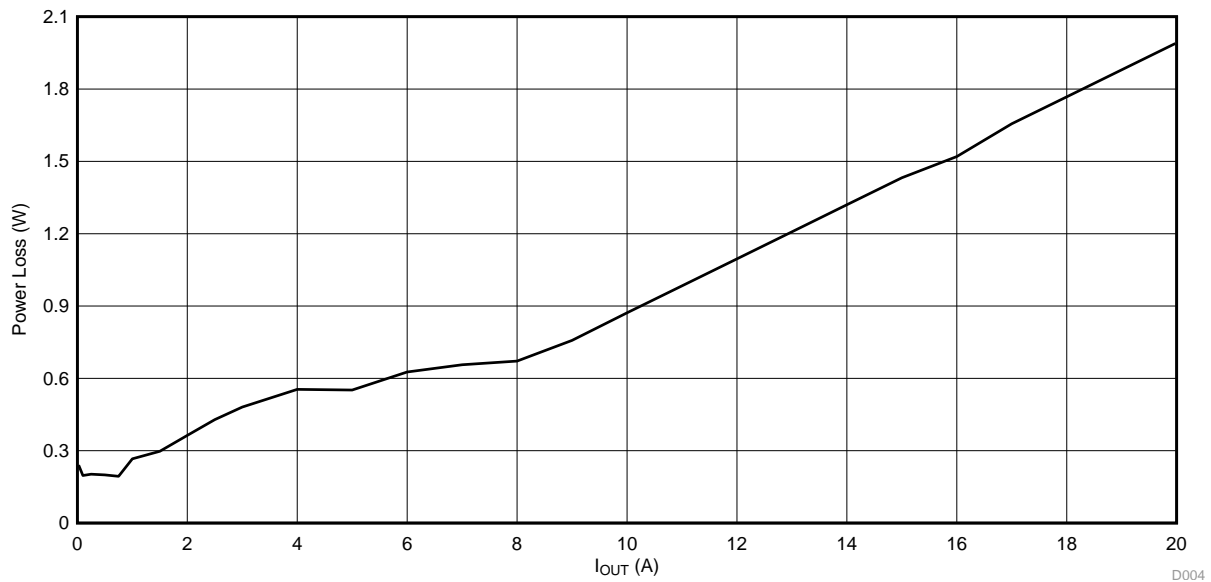


图 5. Auxiliary Rail Power Loss

4.2 Steady-State Regulation and Phase Ringing

Both rails of this design were tested for steady-state stability across their entire load ranges without recording any failures or anomalies. DC ripple remained within the design targets and the measured switching frequency was within the data sheet limits. Care was taken to ensure that the noise floor of the output voltage differential probe did not impact the results to cause false failures in output ripple or stability. TI recommends probing a phase node during testing to check against any possible questions regarding stability that may be attributed to a noisy differential probe. The design is likely stable if the switching frequency is consistent between phase pulses and varies within the TPS53679 data sheet limits. If an adequate differential probe is not available, a passive probe with tight ground connection should be used instead to verify the design.

图 6 和 图 7 显示核心电轨在 100 A 和 200 A 下的测试结果。图 8 和 图 9 显示辅助电轨在 16 A 和 20 A 下的测试结果。

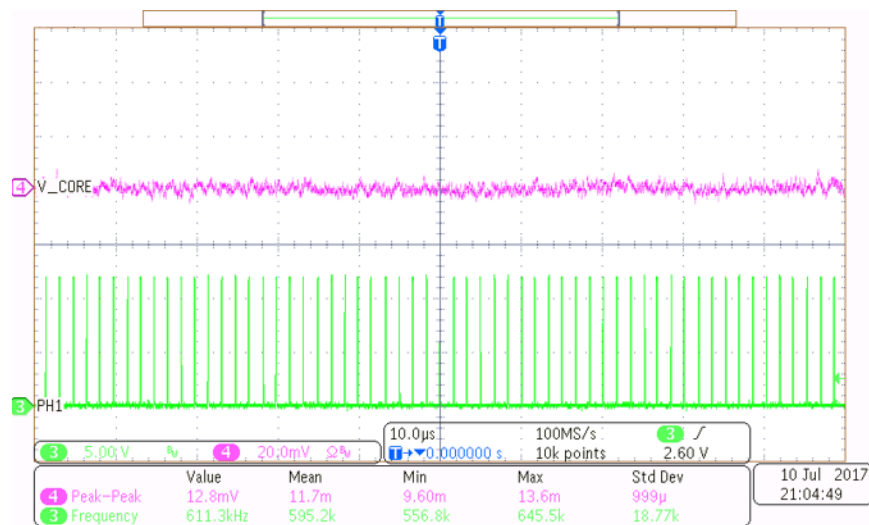


图 6. Core Rail — Steady State, 100 A

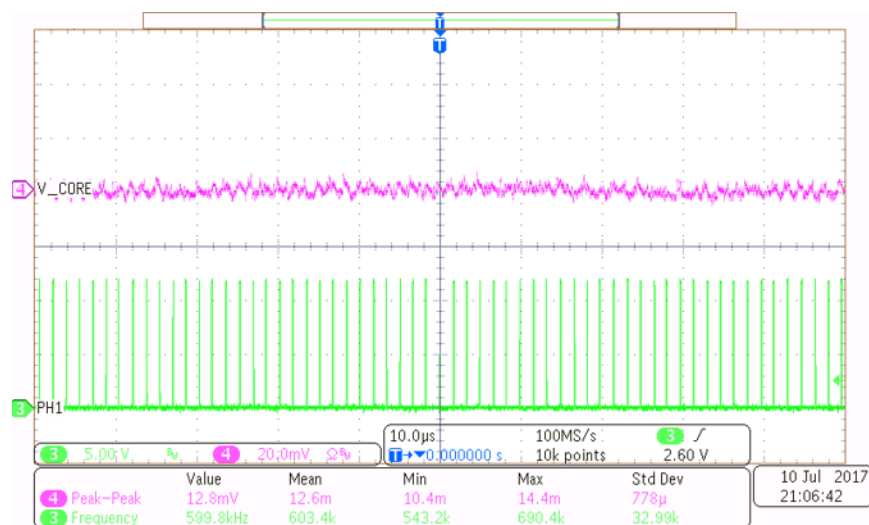
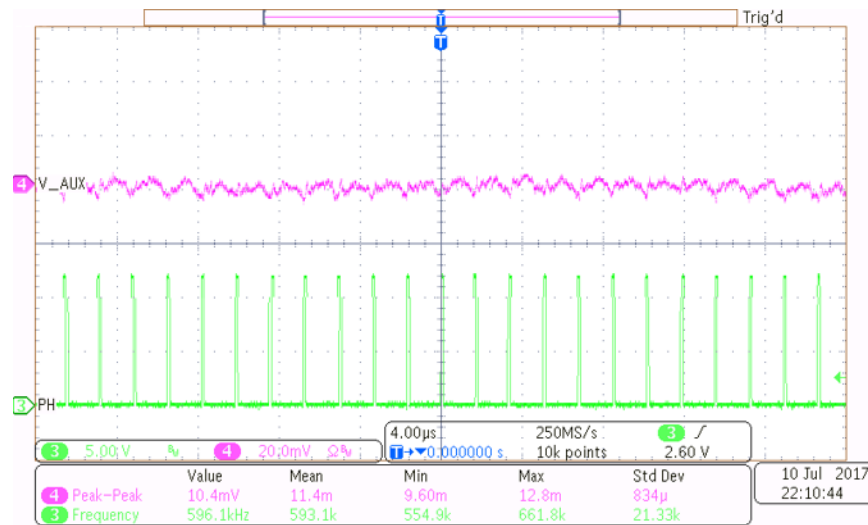
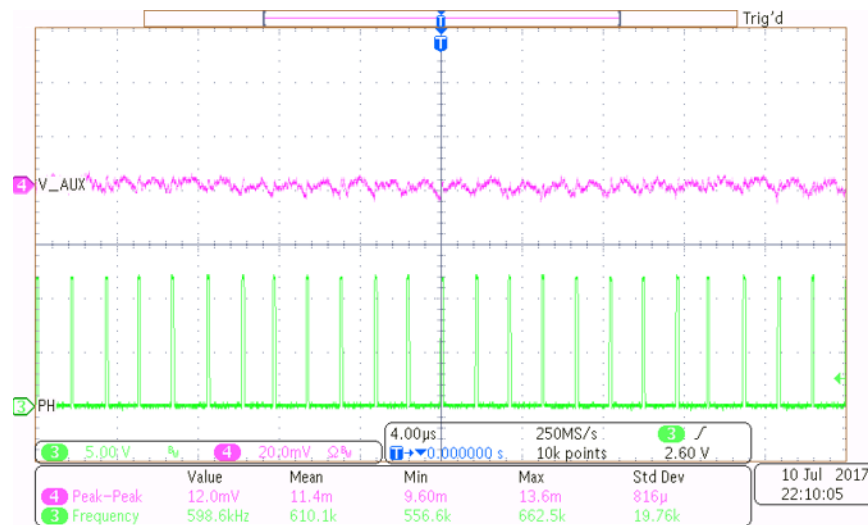


图 7. Core Rail — Steady State, 200 A


图 8. Auxiliary Rail — Steady State, 16 A

图 9. Auxiliary Rail — Steady State, 20 A

To ensure no possible damage to the power MOSFETs, the phase node was measured on the core rail to determine if shoot-through was occurring and if any ringing was within the CSD95490Q5MC data sheet specifications. Without any boot resistor or phase snubber in place, the phase nodes of the rail did not exhibit any issues across the entire load range (see 图 10). However, the impact of several boot resistors and snubbers on efficiency were studied (see 图 11) and the results are summarized in 表 2. If electromagnetic interference (EMI) concerns are present on the end application board, then an appropriate boot resistor or snubber should be used that minimizes the hit on efficiency.

The auxiliary rail showed identical results when tested in the same manner as the core rail.

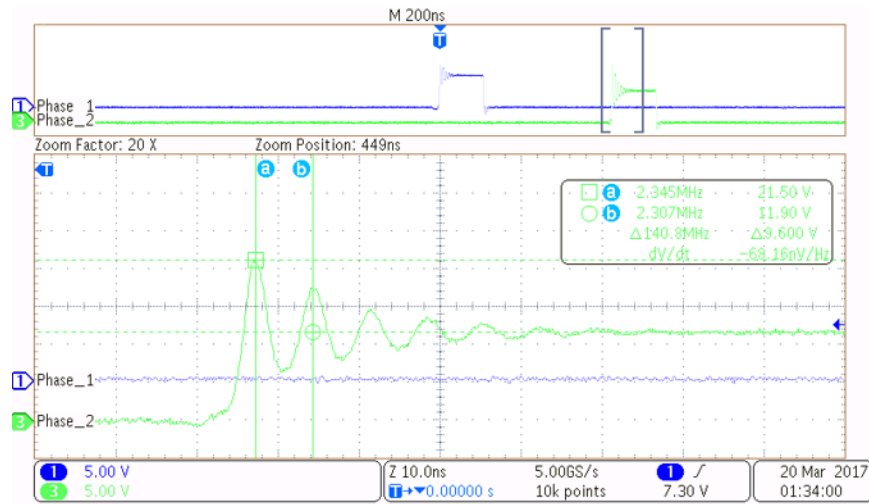


图 10. Phase Ringing — 200 A, No Snubber or Boot Resistor

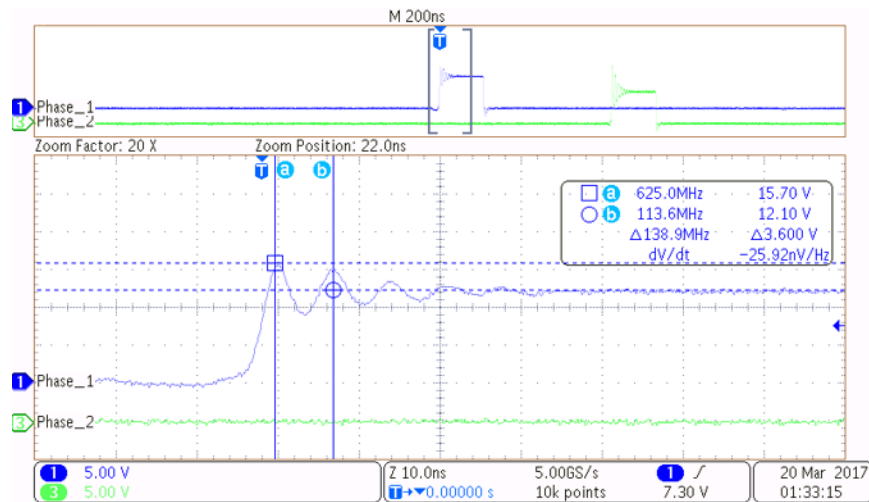


图 11. Phase Ringing — 200-A, 2-Ω Boot Resistor

表 2. Phase Ringing Methods Effects on Efficiency

ADDITIONAL COMPONENTS	EFFICIENCY CHANGE	RINGING OUTSIDE DATA SHEET LIMITS (23 V FOR 10-ns MAX)
None	—	No
2-Ω boot resistor	-1.0%	No
1-Ω boot resistor	-0.5%	No
1-Ω + 1500-pF snubber	-0.75%	No

4.3 Transient Response

A load transient circuit was placed on the board close to the output of the core rail to generate the 150-A step at the fast slew rate of 500 A/ μ s. The single-step response (see 图 12 and 图 13) showed little to no undershoot and the expected 75 mV of droop from the DC loadline while the overshoot was less than the allowable 115 mV. The output voltage remained stable as the load duty cycle was swept from 10% to 80%, as 图 14 shows. Minimal undershoot was once again measured and the overshoot was less than 115 mV. The transient circuit was able to hit the quick slew rate, but it could not handle load frequencies above 200 kHz and so a beat frequency check at 600 kHz could not be performed. However, 图 15 shows that, as the frequency of the load step was swept up to 200 kHz, no instabilities were observed. A few faint traces show the overshoot occasionally exceeds 115 mV at high frequency but this can be mitigated on the end application board by placing small 0402 or 0201 ceramic capacitors between the ASIC power pins. On a demo board such as this, there is not much benefit to placing these capacitors because the distance from their footprints to the load would be too great, which negates their effect.

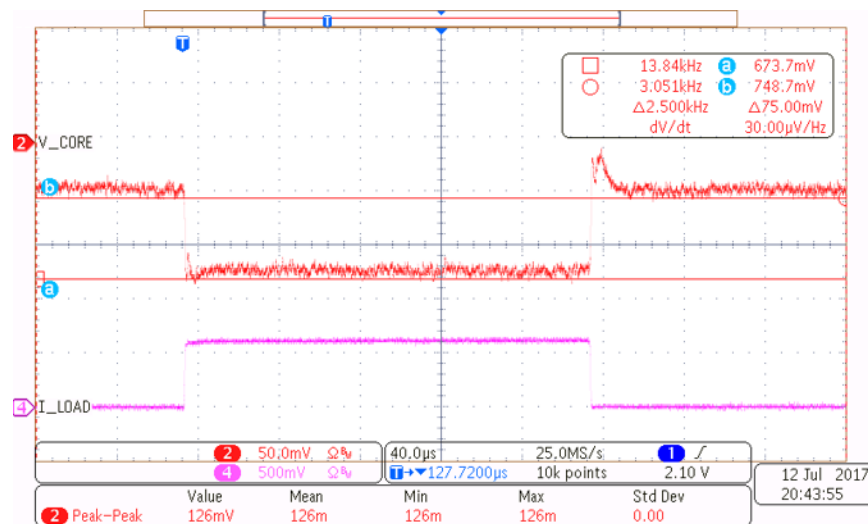


图 12. Core Rail — 90-A to 240-A Transient Undershoot, 20% Duty Cycle

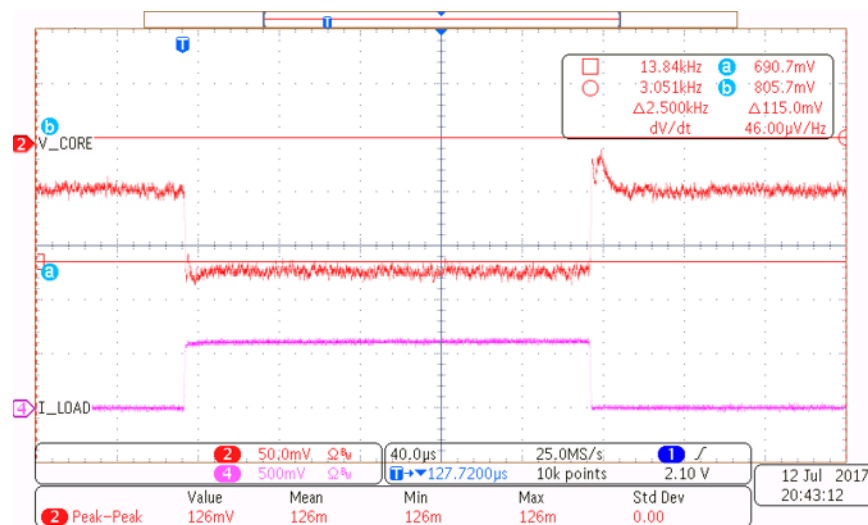


图 13. Core Rail — 90-A to 240-A Transient Overshoot, 20% Duty Cycle

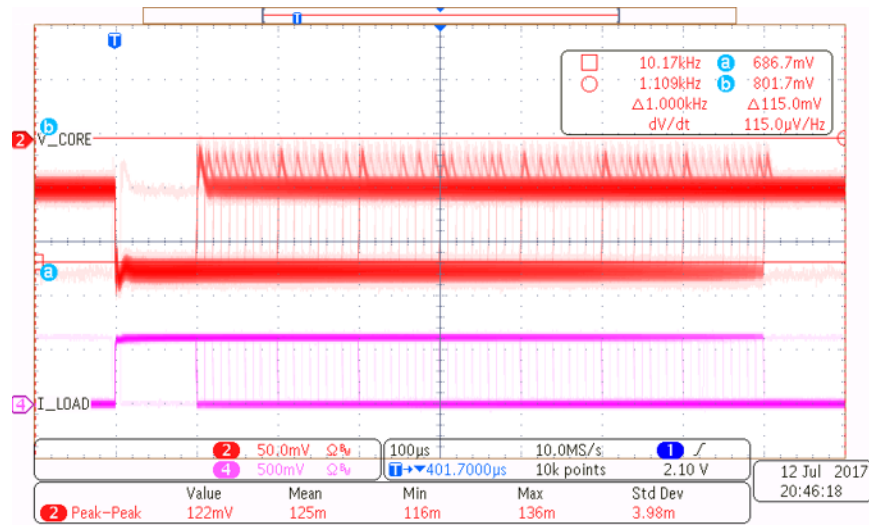


图 14. Core Rail — 90-A to 240-A Transient, 10% to 80% Duty Cycle Sweep

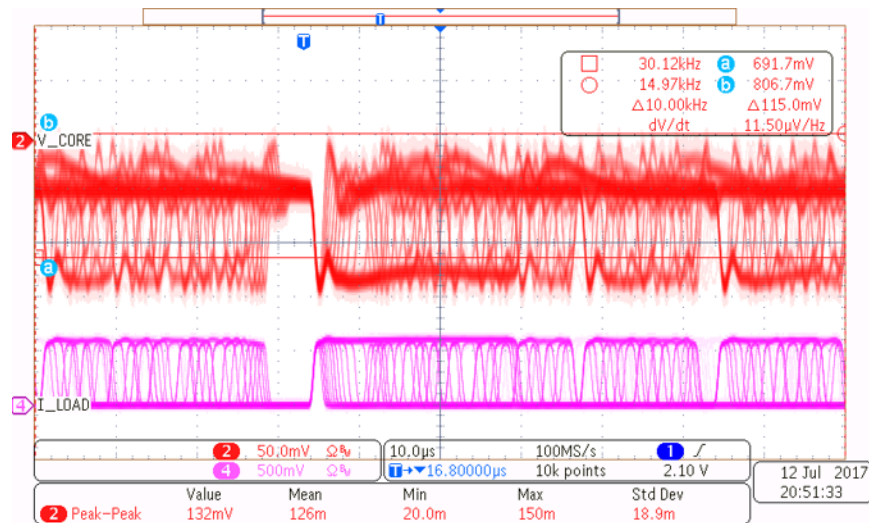


图 15. Core Rail — 90-A to 240-A Transient, 10-kHz to 200-kHz Load Frequency Sweep

A 10-A current step was applied to the auxiliary rail using an external load transient circuit, as the required slew rate was only 20 A/µs (see 图 16). The transient response of the rail was also tested as the load duty cycle (see 图 17) and frequency (see 图 18) were swept across a wide range of values. No instabilities were observed during this sweep and the output voltage remained in its $\pm 5\%$ window around 0.85 V with the exception of some very-high frequency spikes. The spikes are easy to deal with on an end application board using the same method as the core rail with local decoupling using small 0201 or 0402 capacitors. Unlike with the core rail, the load frequency on the auxiliary rail can be swept up to the switching frequency of 600 kHz (see 图 19) to check for beat frequencies. No beat frequencies were recorded and regulation on the output was maintained.

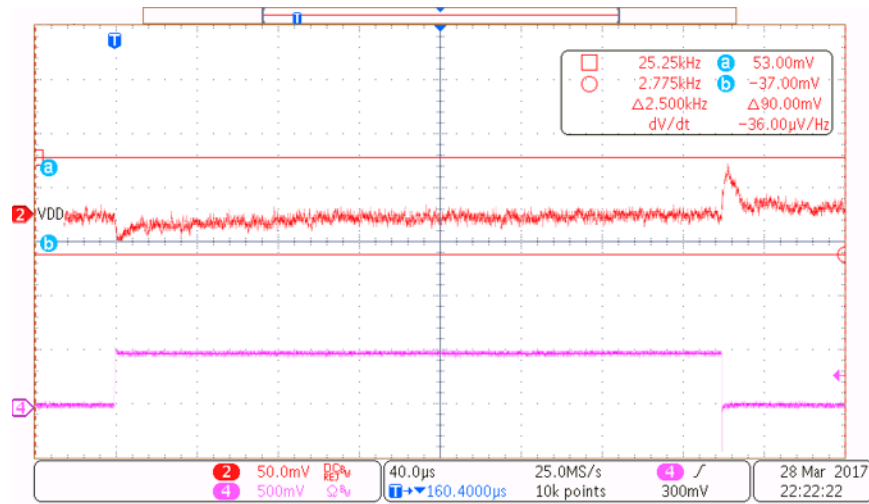


图 16. Auxiliary Rail — 10-A to 20-A Transient, 30% Duty Cycle

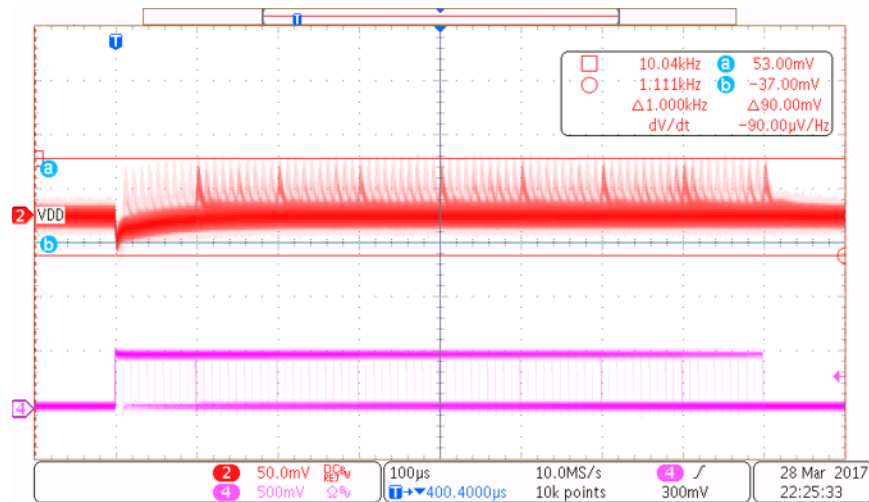


图 17. Auxiliary Rail — 10-A to 20-A Transient, 10% to 80% Duty Cycle Sweep

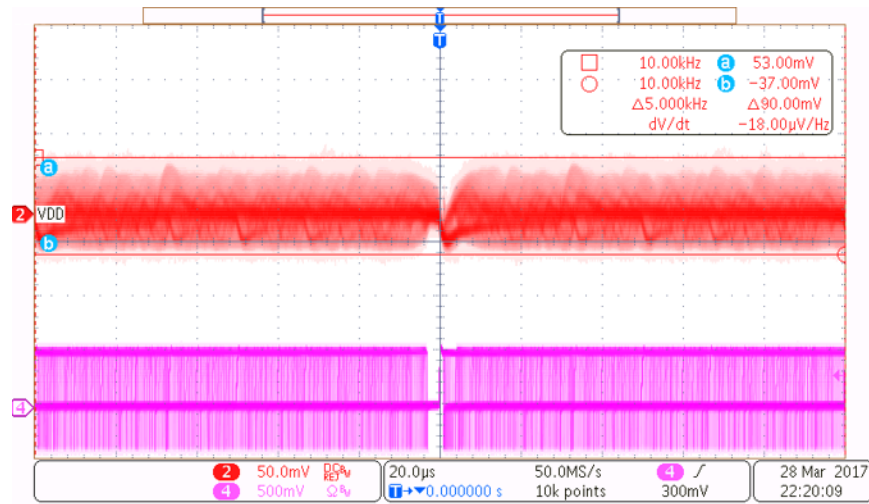


图 18. Auxiliary Rail — 10-A to 20-A Transient, 10-kHz to 200-kHz Load Frequency Sweep

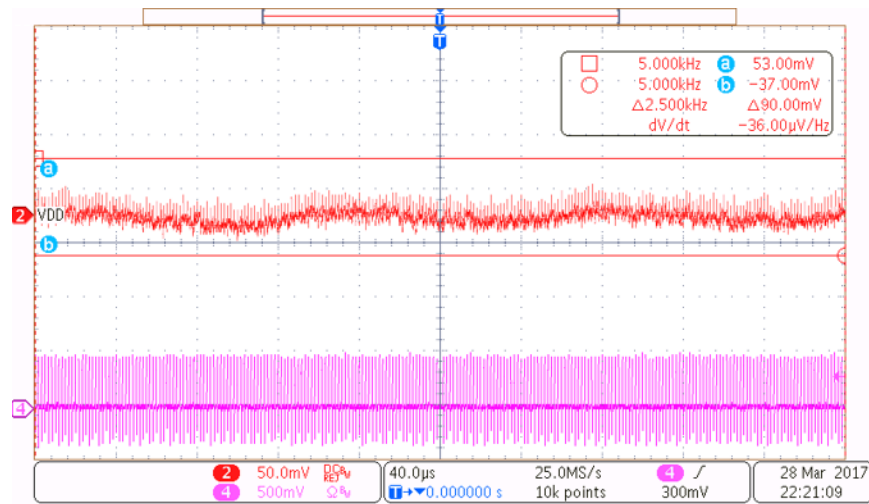


图 19. Auxiliary Rail — 10-A to 20-A Transient, 600-kHz Load Frequency

4.4 Bode Plots

Bode plots for each rail were taken using a network analyzer to determine the transfer function and to check the stability of the control loop for each rail. The core rail has a unity gain frequency of 64 kHz with a phase margin of 71.1°, which indicates stability. Marker 2 of [图 20](#) is placed above the crossover point on a concerning peak in the plot which occurs above the crossover frequency. However, this peak remains well below 0 dB and has no impact on the stability of the core rail.

The auxiliary rail is also stable with a phase margin of 52.7° at a crossover of 79 kHz (see [图 21](#)).

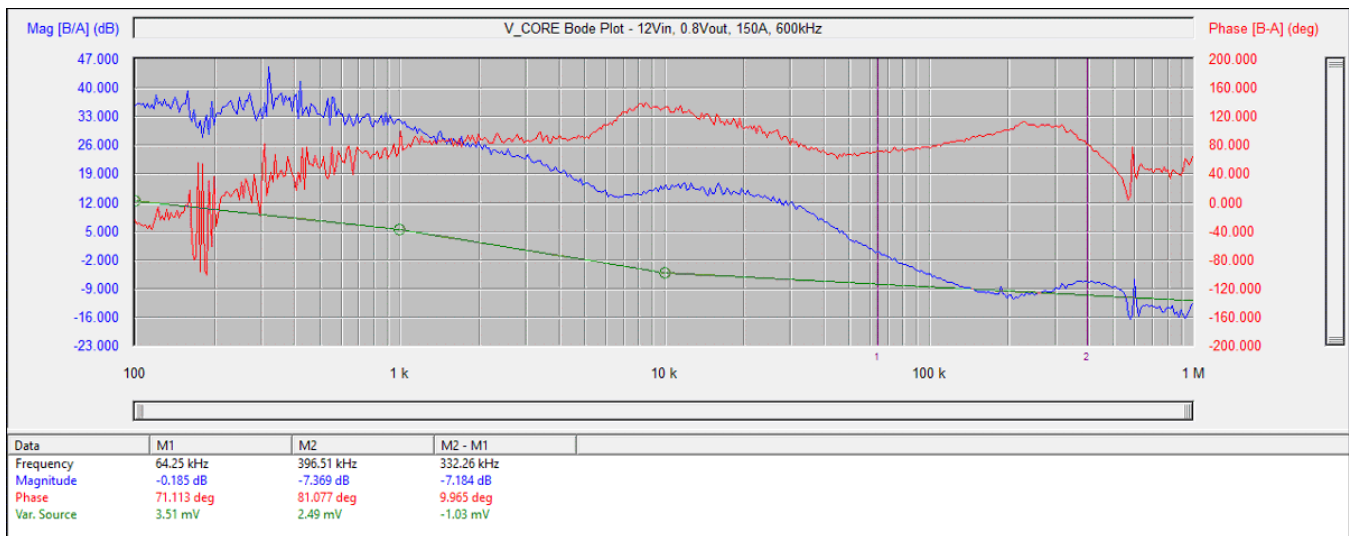


图 20. Core Rail Bode Plot

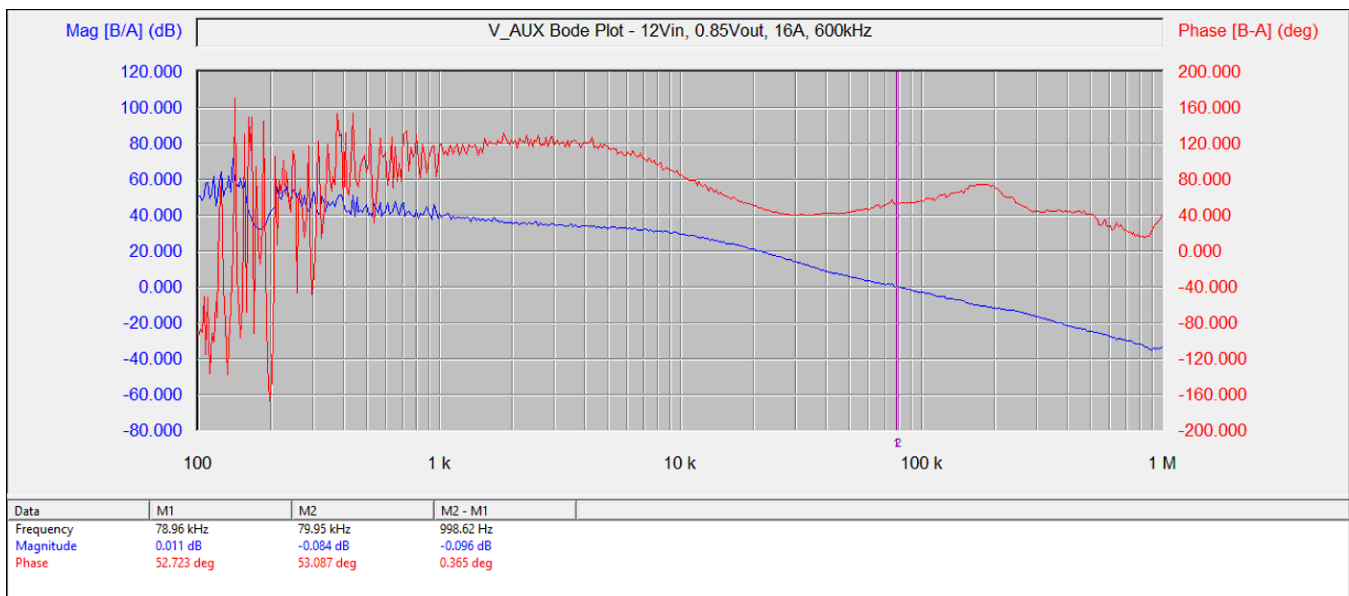


图 21. Auxiliary Rail Bode Plot

4.5 Thermal Performance

The thermal performance of the core rail was tested for 100-A and 200-A loads both with and without airflow. In a real application, a combination of heat sinks and airflow are likely to be used and thus testing without any airflow represents a worst-case scenario. The ambient temperature was 23°C for each test case and the design was allowed to soak for 5 minutes under load to reach thermal equilibrium. A speed of 500 ft/min was used when testing with airflow. As with the steady-state testing, the performance of the electronic load affected the testing and the DC loadline was disabled to obtain the largest possible output load from the equipment.

Performance was significantly increased with airflow. Case temperatures dropped by 10.8°C at 100 A and 20.2°C for 200-A loads.

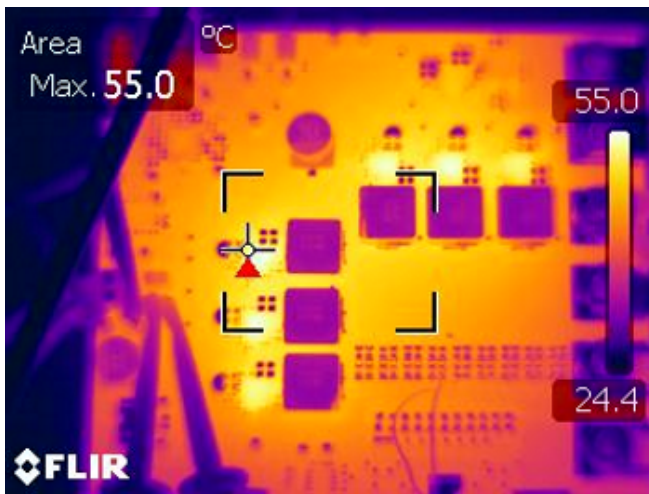


图 22. CSD95490Q5MC Temperature 100-A Load, No Airflow

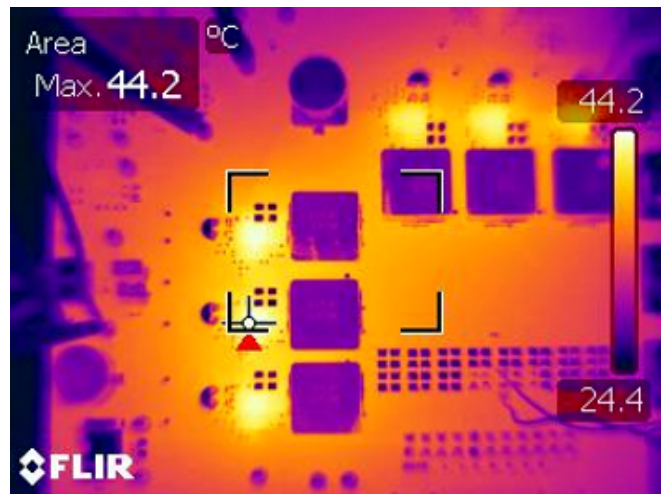


图 23. CSD95490Q5MC Temperature 100-A Load, 500-ft/min Airflow

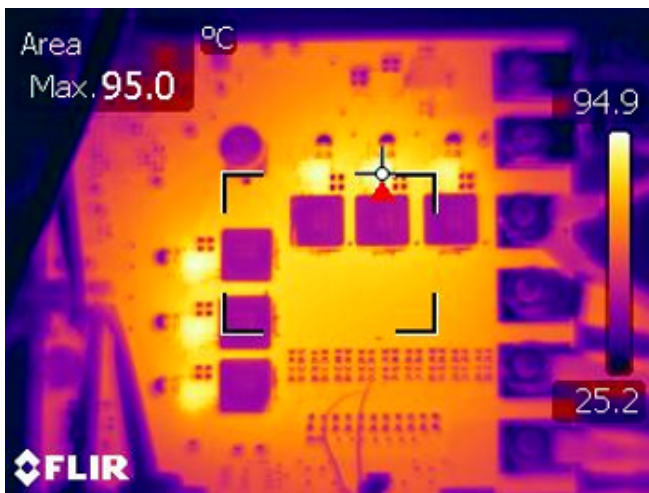


图 24. CSD95490Q5MC Temperature 200-A Load, No Airflow

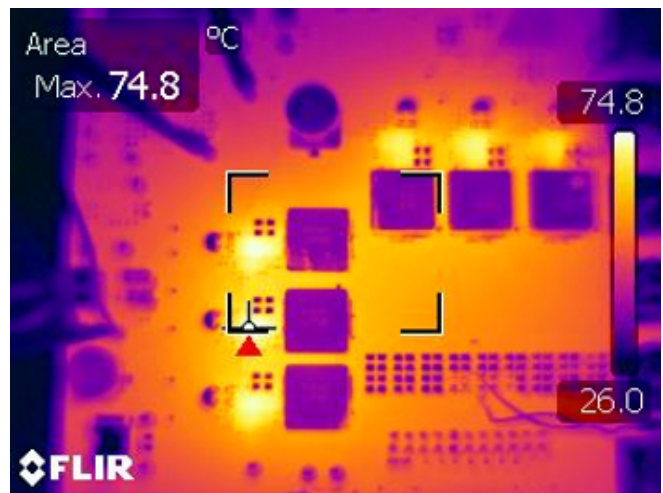


图 25. CSD95490Q5MC Temperature 200-A Load, 500-ft/min Airflow

During the thermal soak a snapshot of the PMBus telemetry was taken using Fusion GUI to check the phase current balancing. In all scenarios, the six-phase currents were within the $\pm 2.5\%$ specifications listed in the power stage data sheet (see 图 26).

PMBus Readings	
Vout:	0.797 V
Pout:	152.00 W
Vin:	11.891 V
Iin:	14.13 A
Pin:	167.50 W
Temp:	65 °C
Iout (Total phases):	190.25 A
Ph1:	31.75 A
Ph2:	32.56 A
Ph3:	31.31 A
Ph4:	31.75 A
Ph5:	30.53 A
Ph6:	33.31 A

图 26. Temperature Monitoring and Phase Current Balancing Seen in Fusion GUI

4.6 Protection Circuitry

The overcurrent and overtemperature protections were tested on both outputs and showed identical performance on each one. Through the PMBus, each rail was configured to shut down for both conditions until the enable pin was toggled. A restart option after 20 ms is also available. When a fault occurs, the controller tri-states the phase node (or multiple phase nodes) and allows the output to decay according to the load current (see 图 27 and 图 29). At the same time, the PGOOD signal is also pulled low to indicate the loss of regulation. During the overcurrent shutdown in 图 27, the output voltage can be observed swinging below ground due to the electronic load trying to maintain the load current. In a real application this action would not occur and V_{CORE} would simply decay to 0 V.

During testing, the status of the system was monitored through Fusion GUI (see 图 28 and 图 30) to check for both the warning and fault flags that are triggered as either the current or temperature exceeds the preset limits. No issues were observed and the part responded per expectations for both overcurrent and temperature shutdown. Note that the trip limits of the rail (as seen in the GUI under test) were lowered to speed up testing, as this was only a basic functionality check.

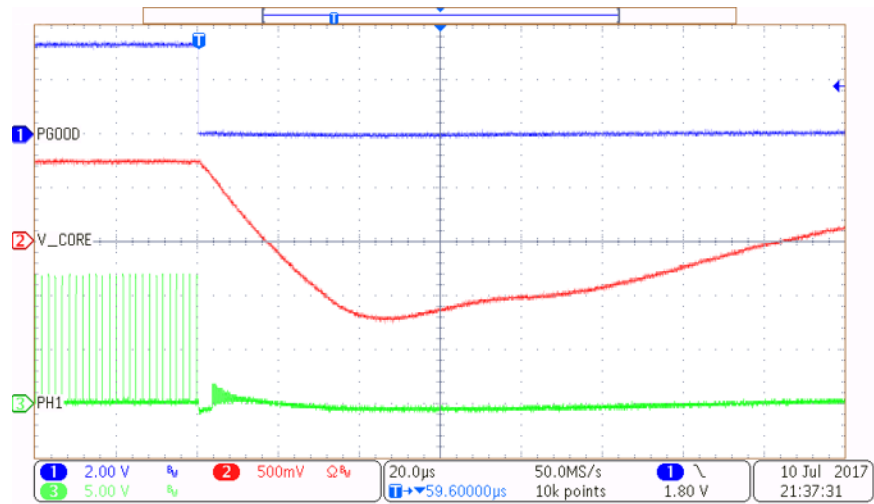


图 27. Overcurrent Shutdown



图 28. Overcurrent Shutdown as Seen in Fusion GUI

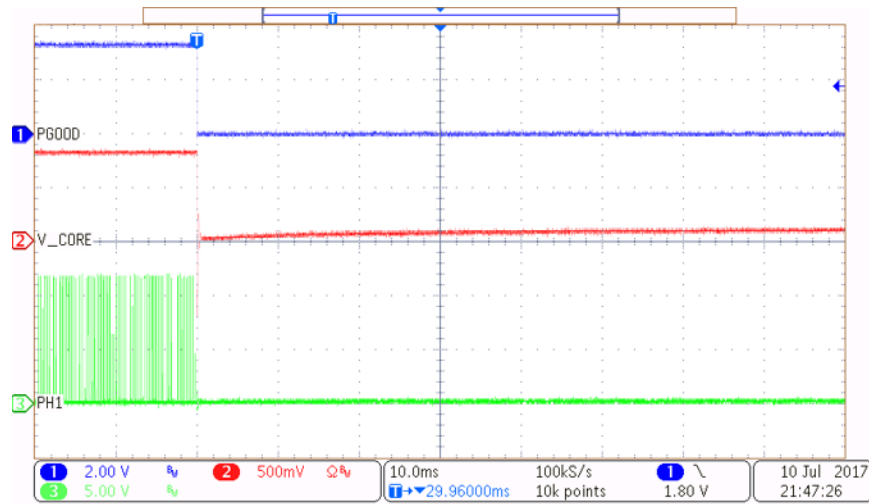


图 29. Overtemperature Shutdown

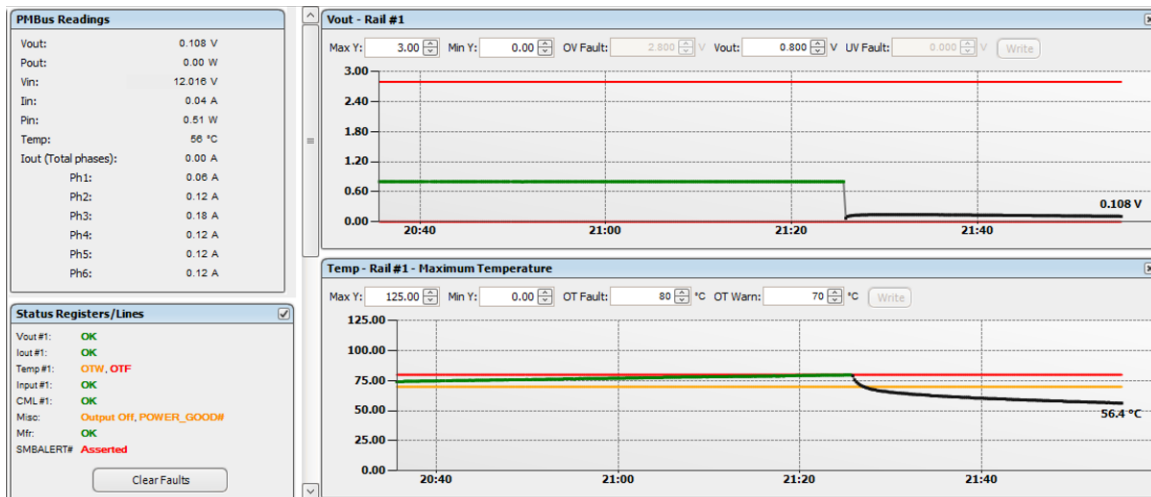


图 30. Overtemperature Shutdown as Seen in Fusion GUI

5 Design Files

5.1 Schematics

To download the schematics, see the design files at [TIDA-01367](#).

5.2 Bill of Materials

To download the bill of materials (BOM), see the design files at [TIDA-01367](#).

5.3 PCB Layout Recommendations

Follow all the layout instructions as specified in the respective data sheet for each part when laying out a design using the TPS53679 controller and CSD95490 Smart Power Stage. Some other guidelines to consider include:

- Keep the layout for all six phases on the core rail identical to ensure optimal current balancing and thermal performance between phases.
- Route noisy traces such as pulse width modulation (PWM) and the PMBus lines on a separate layer than the sensitive analog sense lines such as VSP, VSN, COMP, IMON, and so forth.
- Use quality capacitors for both the input and output decoupling to obtain the maximum performance possible with respect to DC ripple and transient response. Ceramic capacitors must be rated to at least 16 V on V_{IN} and 2.5 V on V_{OUT} with a dielectric rating of X5R or better.
- Ensure that the V_{OUT} and GND nodes are routed on multiple layers of copper and connected with enough vias to handle the current requirements for the best thermal performance. Following this guideline allows for a maximum amount of heat to flow out of the power stages and inductors into the board.

5.4 Gerber Files

To download the Gerber files, see the design files at [TIDA-01367](#).

5.5 Assembly Drawings

To download the assembly drawings, see the design files at [TIDA-01367](#).

6 Software Files

To download the Fusion Digital Power Designer software, see the following [tool folder](#).

7 Related Documentation

1. Texas Instruments, [TPS53679 Dual-Channel \(6-Phase +1-Phase\) or \(5-Phase + 2-Phase\) D-CAP+™ Step-Down Multiphase Controller with NVM and PMBus™ for VR13 Server VCORE](#), TPS53679 Data Sheet (SLUSC47)
2. Texas Instruments, [CSD95490Q5MC Synchronous Buck NexFET™ Smart Power Stage](#), CSD95490Q5MC Data Sheet (SLPS653)

7.1 商标

Fusion Digital Power, PowerPad, NexFET, DualCool are trademarks of Texas Instruments.
Arm is a registered trademark of Arm Limited.
ThunderX2 is a registered trademark of Cavium, Inc.
PMBus is a trademark of SMIF, Inc.
All other trademarks are the property of their respective owners.

8 About the Author

CARMEN PARISI is a Senior Applications Engineer working in the Multiphase and Control Solutions (MCS) group at TI developing reference designs and application notes. He has six years of experience in power electronics working on mobile, desktop, and server V_{CORE} applications; battery chargers; and system PMICs. Carmen earned a combined BS/MS degree in electrical engineering from the Rochester Institute of Technology.

修订历史记录

注：之前版本的页码可能与当前版本有所不同。

Changes from Original (August 2017) to A Revision	Page
• 已更改 将设计标题从采用 <i>TPS53679</i> 且适用于联网 ASIC 的高功率 6+1 稳压器参考设计 改为采用 <i>Cavium ThunderX2®</i> <i>Arm®</i> 处理器的高功率稳压器参考设计	1

重要声明和免责声明

TI 均以“原样”提供技术性 & 可靠性数据（包括数据表）、设计资源（包括参考设计）、应用或其他设计建议、网络工具、安全信息和其他资源，不保证其中不含任何瑕疵，且不做任何明示或暗示的担保，包括但不限于对适销性、适合某特定用途或不侵犯任何第三方知识产权的暗示担保。

所述资源可供专业开发人员应用 TI 产品进行设计使用。您将对以下行为独自承担全部责任：(1) 针对您的应用选择合适的 TI 产品；(2) 设计、验证并测试您的应用；(3) 确保您的应用满足相应标准以及任何其他安全、安保或其他要求。所述资源如有变更，恕不另行通知。TI 对您使用所述资源的授权仅限于开发资源所涉及 TI 产品的相关应用。除此之外不得复制或展示所述资源，也不提供其它 TI 或任何第三方的知识产权授权许可。如因使用所述资源而产生任何索赔、赔偿、成本、损失及债务等，TI 对此概不负责，并且您须赔偿由此对 TI 及其代表造成的损害。

TI 所提供产品均受 TI 的销售条款 (<http://www.ti.com.cn/zh-cn/legal/termsofsale.html>) 以及 [ti.com.cn](http://www.ti.com.cn) 上或随附 TI 产品提供的其他可适用条款的约束。TI 提供所述资源并不扩展或以其他方式更改 TI 针对 TI 产品所发布的可适用的担保范围或担保免责声明。

邮寄地址：上海市浦东新区世纪大道 1568 号中建大厦 32 楼，邮政编码：200122
Copyright © 2018 德州仪器半导体技术（上海）有限公司

重要声明和免责声明

TI 均以“原样”提供技术性 & 可靠性数据（包括数据表）、设计资源（包括参考设计）、应用或其他设计建议、网络工具、安全信息和其他资源，不保证其中不含任何瑕疵，且不做任何明示或暗示的担保，包括但不限于对适销性、适合某特定用途或不侵犯任何第三方知识产权的暗示担保。

所述资源可供专业开发人员应用 TI 产品进行设计使用。您将对以下行为独自承担全部责任：(1) 针对您的应用选择合适的 TI 产品；(2) 设计、验证并测试您的应用；(3) 确保您的应用满足相应标准以及任何其他安全、安保或其他要求。所述资源如有变更，恕不另行通知。TI 对您使用所述资源的授权仅限于开发资源所涉及 TI 产品的相关应用。除此之外不得复制或展示所述资源，也不提供其它 TI 或任何第三方的知识产权授权许可。如因使用所述资源而产生任何索赔、赔偿、成本、损失及债务等，TI 对此概不负责，并且您须赔偿由此对 TI 及其代表造成的损害。

TI 所提供产品均受 TI 的销售条款 (<http://www.ti.com.cn/zh-cn/legal/termsofsale.html>) 以及 [ti.com.cn](http://www.ti.com.cn) 上或随附 TI 产品提供的其他可适用条款的约束。TI 提供所述资源并不扩展或以其他方式更改 TI 针对 TI 产品所发布的可适用的担保范围或担保免责声明。

邮寄地址：上海市浦东新区世纪大道 1568 号中建大厦 32 楼，邮政编码：200122
Copyright © 2018 德州仪器半导体技术（上海）有限公司